ADAPTIVE SOLUTIONS OF NONLINEAR PARABOLIC EQUATIONS WITH APPLICATION TO HYPERTHERMIA TREATMENTS

Bodo Erdmann, Jens Lang, Martin Seebaß
Konrad-Zuse-Zentrum für Informationstechnik Berlin
Takustraße 7
14195 Berlin - Dahlem, Federal Republic of Germany
erdmann@zib.de

ABSTRACT. We present a self-adaptive finite element method to solve nonlinear evolution problems in 3D. An implicit time integrator of Rosenbrock type is coupled with a multilevel approach in space. The proposed method is applied to hyperthermia treatments to demonstrate its potential for the solution of complicated problems.

INTRODUCTION

Many phenomena in biology, chemistry, physics, and engineering are set up by time-dependent systems of PDEs which have to be solved numerically under increasingly complex conditions. Typically, the solutions have a dynamic behaviour in space and time. In such a situation only adaptive methods are able to control efficiently discretization errors with respect to required tolerances and computational work.

Adaptive hierarchical finite element methods have been developed by the authors to solve problems with highly non-uniform solutions[1,2,3]. The proposed methods are essentially based on the repeated application of solving discretized equations, error estimation, and local refinement. The final spatial grids are well adapted to the required solution. The reliability of the algorithm has been demonstrated for a variety of chemical problems known to range among the most demanding for spatial adaptivity when thin flame fronts are to be resolved numerically[4].

To include more challenging practically relevant problems we extended the above techniques to three-dimensional problems using Finite Elements in space and Rosenbrock methods for temporal discretization[5]. Error estimates utilize embedding in time and hierarchical bases in space. Dynamic tree structures are employed to manage grid enhancement and robust coarsening as well.

We apply our method in the field of medical planning for simulation of hyperthermia treatments. Hyperthermia, i.e. heating of tissue, is a method of cancer therapy. In most cases electromagnetic waves are used as heat source. Our model of heat transfer within the human body is Pennes' bio-heat-transfer equation (BHTE)

$$\rho\, c\, \partial T/\partial t = \nabla(\kappa\, \nabla T) - c_b\, W\, (T-T_b) + ARD \qquad (1)$$

with the density ρ, the specific heat c, the thermal conductivity κ, the blood perfusion W, and the temperature T. The index b is related to blood. The source term ARD describes the absorbed power per volume of the electric field. Boundary conditions are obtained from

$$\kappa\, \partial T/\partial n = h\, (T_{out} - T), \qquad (2)$$

where T_{out} is the environmental temperature, and h is the heat transfer coefficient. The main assumption of this model is that the blood enters the local tissue with the body core temperature and leaves it with the local tissue temperature. Hence, convective heat flow can be described by the temperature difference $T-T_b$ and an empirical transfer coefficient c_b W.

For a patient-specific simulation we generate a three-dimensional finite element mesh in which the relevant tissue compartments are represented. Mesh generation is based on a set of computer tomographic scans of the patient[7]. A discretized part of a patient lying in a radiofrequency hyperthermia applicator is shown in Fig. 1.

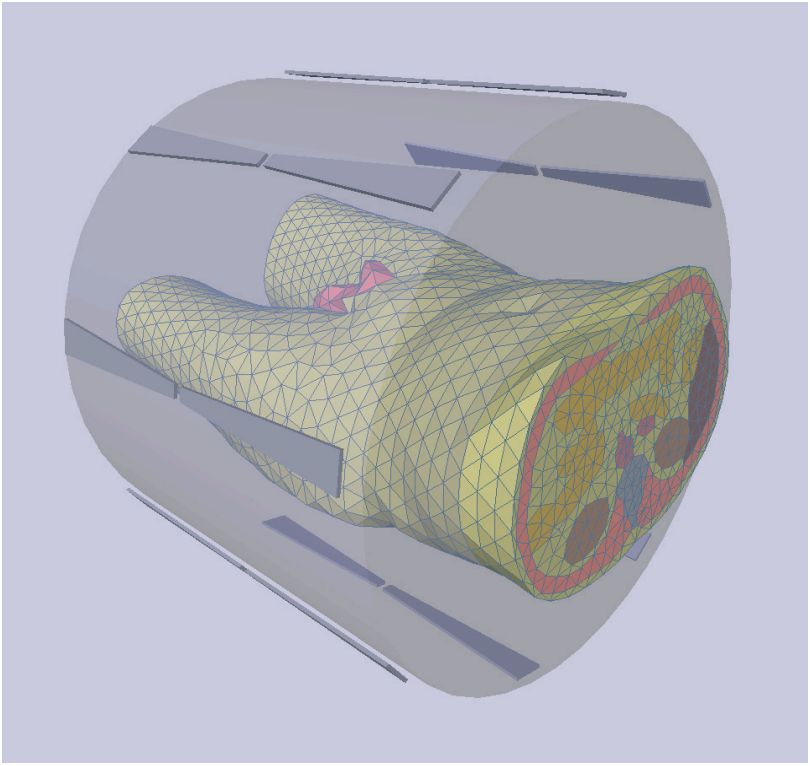

Fig.1: Finite element model for a patient.

We compare a linear temperature model of the BHTE (constant perfusion W within each tissue compartment) with a nonlinear version (temperature-dependent perfusion). Several simulations reveal that the temperature at the steady state is significantly higher with a temperature-dependent perfusion. This observation is comparable with the results reported for a 2D-simulation of hyperthermia induced by ferromagnetic seeds[8] .

Furthermore, spatial adaptivity allows us to get efficiently more accurate solutions necessary for reliable decisions in medical planning.

Besides the study of the stationary solution, we are interested in gaining an insight into the evolution of body heating.

The implementation of finite element codes in three space dimensions employing adaptive mesh refinement and multilevel techniques requires modern software design and programming languages as C or C++. Our code KARDOS is based on the programming environment KASKADE[1]. Additionally, a comfortable visualization tool is invaluable. We used the graphical system HyperPlan[10] for the presentation of our numerical results.

MATHEMATICAL MODELLING OF BLOOD PERFUSION

Studies that predict temperatures in tissue models usually assume a constant-rate blood perfusion within each tissue. However, several experiments have shown that the response of vasculature in tissues to heat stress is strongly temperature-dependent[8]. When heated the blood flow in normal tissues, e.g., skin and muscle, increases significantly. In contrast, the tumor zone often appears to be so vulnerable to heat that the blood flow decreases upon heating.

Our models of temperature-dependent blood perfusion in the muscle and tumor are derived from special curves propagated by Tompkins[8]. We fit the curves employing our constant blood perfusions (Tab.1). Additionally, we apply a nonlinear perfusion model for fat tissue related to that of muscle. The expressions for evaluating the blood perfusion W are:

Nonlinear blood perfusion in muscle:

$$W_{muscle} = 4.0 - 1.0723\,(T-45.0)^4\,, \qquad 44.0 <= T <= 46.0$$
$$W_{muscle} = 0.833 + 2.276\,\exp(-(T-45.0)^2/12.0)\,, \qquad T < 44.0,\ T > 46.0$$

Nonlinear blood perfusion in fat:

$$W_{fat} = 0.72 - 0.0682\,(T-45.0)^4\,, \qquad 44.0 <= T <= 46.0$$
$$W_{fat} = 0.36 + 0.317\,\exp(-(T-45.0)^2/12.0)\,, \qquad T < 44.0,\ T > 46.0$$

Nonlinear blood perfusion in tumor:

$$W_{tumor} = 0.833, \qquad T < 37.0$$
$$W_{tumor} = 0.833 - (T-37.0)^{4.8}/6.21e{+}3, \qquad 37.0 <= T <= 42.0$$
$$W_{tumor} = 0.468, \qquad T > 42.0.0$$

Two different simulations are performed. Firstly, we assume that blood perfusion is independent of temperature. Then we incorporate the temperature-dependent models for muscle, fat, and tumor, while the other blood perfusions remain unchanged.

Tissue	Thermal conductivity κ [W/m/^{o}C]	Density ρ [kg/m^3]	Specific heat c [W s/kg/ ^{o}C]	Constant perfusion W [kg/s/m^3]	Nonlinear perfusion W [kg/s/m^3]
Fat	0.210	900	3,500	0.720	W_{fat}
Tumor	0.642	1,000	3,500	0.833	W_{tumor}
Bladder	0.600	1,000	3,500	5.000	5.000
Kidney	0.577	1,000	3,500	66.670	66.670
Liver	0.640	1,000	3,500	16.670	16.670
Muscle	0.642	1,000	3,500	4.000	W_{muscle}
Bone	0.436	1,600	1,000	1.333	1.333
Aorta	0.506	1,000	3,500	83.330	83.330
Intestine	0.550	1,000	3,500	3.333	3.333

Table 1: Material properties of tissues.

The material properties of the involved tissues are summarized in Table 1. In the temperature-independent case they are assumed to be independent of temperature over the hyperthermic temperature range and are considered uniform throughout each tissue type. For the simulation we further set $T_b = 37^oC$, $c_b = 3500$ Ws/kg/^{o}C, $h = 45$ W/m^2/^{o}C, and $T_{out} = 25^oC$.

ADAPTIVE TIME AND SPACE DISCRETIZATION

The principle difficulties in numerically solving the bio-heat transfer equation are the nonlinearity due to the perfusion term and the different material properties of the tissues. Using a linearly implicit method of Rosenbrock type for the time discretization, we are able to integrate the heat equation efficiently. Within this approach, the approximate temperature T_n at time t_n is constructed by a linear combination of the previous temperature T_{n-1} at time t_{n-1} and different intermediate values ΔT_n^j, j=1,2,3, namely

$$T_n = T_{n-1} + \sum_{j=1(1)3} b_j \Delta T_n^j . \tag{3}$$

These values ΔT_n^j are determined by the following linear elliptic boundary value problems:

$$\rho\, c / (\gamma \Delta t_n)\, \Delta T_n^j - \mathrm{div}(\kappa\, \mathrm{grad}\, \Delta T_n^j) + c_b\, JF[T_{n-1}]\, \Delta T_n^j =$$

$$\mathrm{div}(\kappa\, \mathrm{grad}\, T_n^j) - c_b\, F[T_n^j] + \rho\, c / \Delta t_n \sum_{i=1(1)j-1} c_{ji}\, \Delta T_n^i + ARD \text{ in } \Omega, \tag{4}$$

$$\kappa\, \partial(\Delta T_n^j)/\partial n = h\, (T_{out} - \Delta T_n^j) \text{ on } \partial\, \Omega \tag{5}$$

with

$$T_n^j := T_{n-1} + \sum_{i=1(1)j-1} a_{ji}\, \Delta T_n^i\, ,\ \Delta t_n := t_n - t_{n-1},$$

$$F := W(T - T_b),\ JF := \partial F/\partial T.$$

The solution process for the intermediate temperatures ΔT_n^j can be done successively because the sums in the right-hand side of (4) extend to j-1 only. The coefficients γ, a_{ji}, c_{ji}, and b_j are chosen such that the method reaches order three and has good stability properties[6].

The special structure of the employed Rosenbrock method (3) allows us to define a solution of second order T_n^* only using a different set of coefficients b_j^* in (3). The difference between the two solutions $\| T_n - T_n^* \| =: \in_n$ satisfactorily estimates the local error of the time discretization, and can be utilized to propose a new time step

$$\Delta t_{n+1} = (TOL_t/\in_n)^{1/3}\ \Delta t_n.$$

This step size selection guarantees that the stationary solution is reached in a few steps with respect to a desired tolerance TOL_t.

The linear elliptic problems (4) have to be solved for each intermediate value ΔT_n^j. Employing directly our tetrahedral grid, a natural choice is a continuous finite element discretization in space. This method ensures automatically the continuity of the temperature and its fluxes at the inner tissue boundaries.

The starting point of the finite element method is the weak formulation of (4). Let S_h^1 consist of all continuous functions which are polynomials of first order on each finite element, then the finite element solutions $\Delta_h T_n^j \in S_h^1$ have to satisfy the equations

$$(A_n\ \Delta_h T_n^j, \phi) = (r_n^j, \phi) \qquad \forall\ \phi \in S_h^1,\ j = 1,2,3.$$

Here, (. , .) represents the usual inner product, A_n is the weak representation of the differential operator at the left-hand side in (4) and includes the boundary conditions. The function r_n^j stands for the whole right-hand side of the j-th equation in (4). The operator A_n is independent of j, so that the method requires ist calculation only once within each time step.

To get a posteriori error estimates for the spatial discretization, we solve local Dirichlet problems on small subdomains. Let Q_ω be the set of all quadratic polynomials over ω which is the union of all tetrahedra having one common edge. Because we solve our elliptic problems (4) using linear elements, the local approximation of the spatial errors $\Delta T_n^j - \Delta_h T_n^j$ should be computed with at least the basis functions of Q_ω. Imposing homogeneous Dirichlet boundary conditions, the local approximate errors related to all ω are represented by one degree of freedom at the midpoint of the corresponding edge. These local a posteriori error estimates are employed to decide which elements to refine or to unrefine. The aim of our mesh adaptation is to equilibrate the error until a final mesh is created in which all elements have approximately the same error, and a global prescribed tolerance TOL_x is reached.

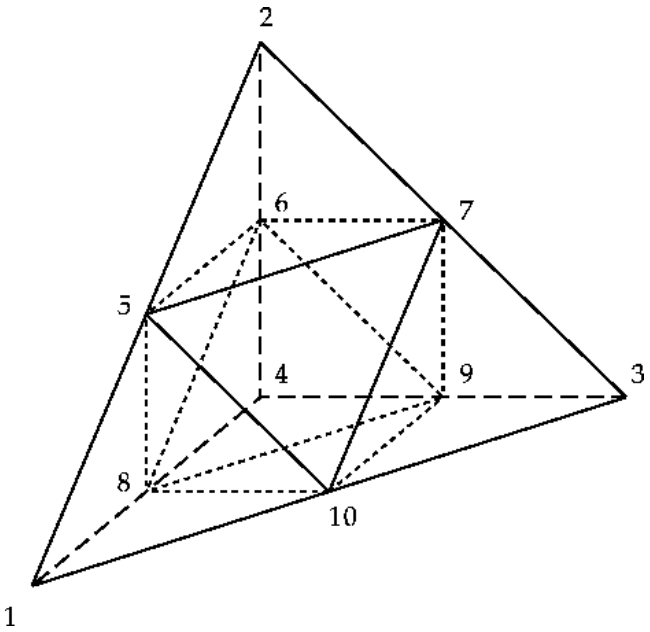

Fig. 2: Regular refinement of a tetrahedron.

For local mesh refinements we use regular partitions of tetrahedra. By connecting the midpoints of the edges of a given tetrahedron, as shown in Fig.2, we obtain four new tetrahedra each of which corresponds to a vertex. The remaining octahedron is splitted into four more tetrahedra. Special closures are applied to ensure conforming triangulations[2].

RESULTS

1. *Constant model versus nonlinear model*. Results from a simulation with constant-rate blood perfusion are compared with those of temperature-dependent blood perfusion applying no grid improvements. The maximum tissue temperatures at the steady state are up to 2.7°C higher in the nonlinear case. In contrast, the minimum tissue temperatures are slightly lower except for tumor and bone. It can clearly be seen that the tumor temperature rises higher than temperatures in normal tissue when the blood flow in normal tissue becomes greater than that in the tumor (Tab.2).

Tissue	T_{max}			T_{min}		
	Linear Coarse	Nonlinear Coarse	Nonlinear Adaptive	Linear Coarse	Nonlinear Coarse	Nonlinear Adaptive
Fat	44.7	46.6	46.8	26.9	26.7	27.1
Tumor	45.9	48.6	48.8	38.3	40.0	40.2
Bladder	43.1	43.9	44.9	37.3	37.3	37.4
Kidney	37.3	37.5	37.7	37.0	36.9	36.9
Liver	37.3	37.2	37.2	36.9	36.7	36.6
Muscle	44.7	45.4	45.0	30.5	29.1	28.9
Bone	43.9	44.9	44.7	36.9	36.3	35.8
Aorta	39.0	39.7	40.3	36.7	36.5	36.5
Intestine	42.9	43.3	43.8	36.9	36.1	36.0

Table 2: Maximum and minimum temperatures of tissues.

2. *Coarse grid versus adaptive grid*. The stationary temperature distribution from a simulation with temperature-dependent blood perfusion using the coarse grid is compared with the stationary temperature field computed with an adaptively improved spatial grid. We observe significant differences in the tissue temperatures. For example, the maximum temperature increases by 1°C in the bladder and decreases by 0.4°C in the muscle tissue.

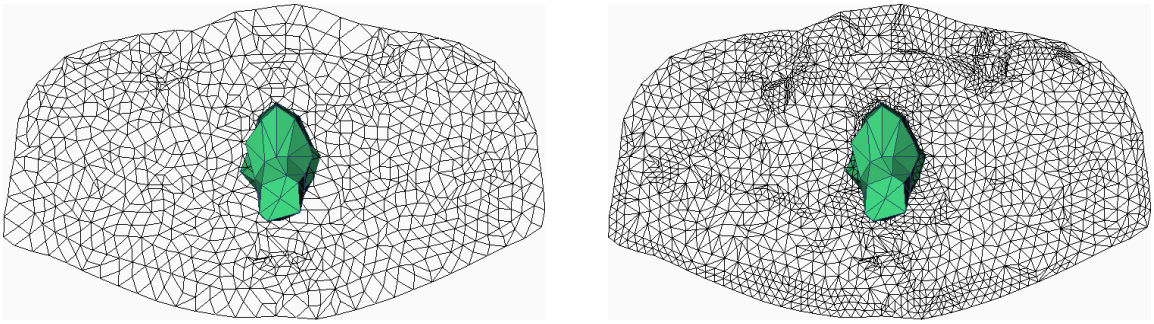

Fig.3: Coarse and refined grid with tumor boundary.

Fig.3 shows two cuts through the computational domain involving the tumor boundary to give an impression of the local refinement process. The whole solution of the coarse grid is evaluated with 8,416 degrees of freedom, while the refined grid has 103,233 degrees of freedom. Starting with the coarse grid three refinement steps are necessary to reach a tolerance of 2%. The corresponding uniform grid would have about 3,000,000 degrees of freedom which demonstrates the power of the proposed adaptive method. We note that local refinement controlled by a posteriori error estimates leads to a better resolution of the solution in regions with high temperature gradients and material transitions.

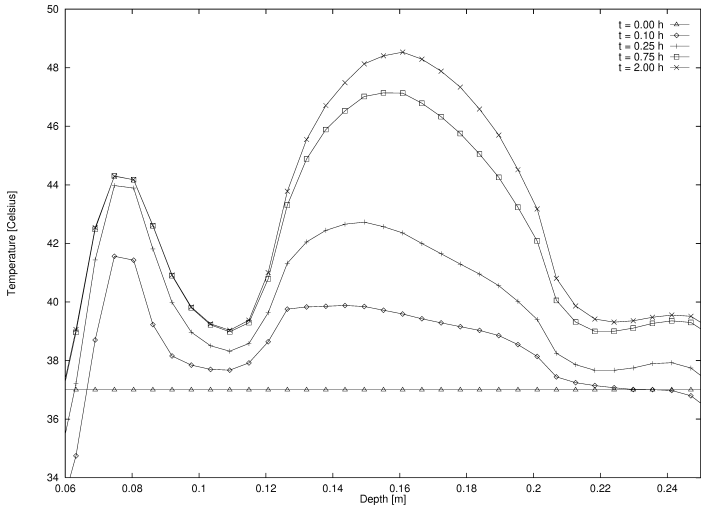

Fig.4: Evolution of temperature along a line.

3. *Evolution of temperature.* To give an impression of the unsteady solution process, we have plotted the temperature distribution along a special line through the body at several times, see Fig. 4. The results are obtained employing the nonlinear perfusion model solved by our adaptive approach. The computation starts with T = 37°C and reaches the steady

state after approximately two hours. The local maximum near the left boundary (located in the hip bone) appears rapidly while the heating of the tumor (in the middle of the picture) takes more time.

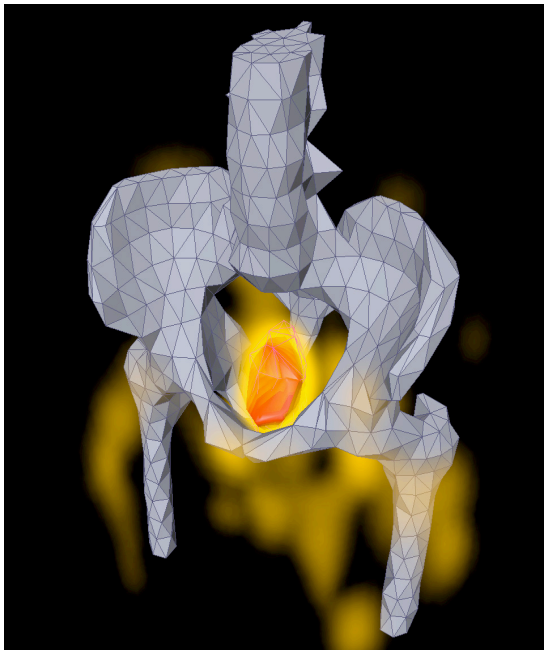

Fig.5: Optimized temperature distribution.

The proposed numerical method is used to optimize the electric field in order to ensure an effective cancer therapy. The solution of such an optimized problem is shown in Fig.5.

ACKNOWLEDGEMENT
The authors are indebted to P. Deuflhard for his continuing support of this project.

REFERENCES

1. Erdmann, B., Lang, J., Roitzsch, R., KASKADE-Manual, Technical Report TR 93-5, Konrad-Zuse-Zentrum für Informationstechnik Berlin, Germany, 1993.

2. Bornemann, F., Erdmann, B., Kornhuber, R., Adaptive multilevel methods in three space dimensions, Int. J. Num. Meth. Engrg., Vol. 36, pp 3187 - 3203, 1993.

3. Lang, J., Two-dimensional fully adaptive solutions of reaction-diffusion equations, Appl. Numer. Math., Vol. 18, pp 223 - 240, 1995.

4. Lang, J., High-Resolution Self-Adaptive Computations on Chemical Reaction-Diffusion Problems with Internal Boundaries, Chem. Engrg. Sci., Vol.51, pp 1055 - 1070, 1996.

5. Lang, J., Roitzsch, R., Erdmann, B., Three-Dimensional Fully Adaptive Solution of Thermo--Diffusive Flame Propagation Problems. In R. W. Lewis (ed.), Proc. of the 10th Int. Conf. on Numer. Meth. in Thermal Probl., Swansea, pp 857-862 , 1997.

6. Roche, M., Rosenbrock methods for differential algebraic equations. Numer. Math., Vol.52, 45 -63, 1988.

7. Seebaß, M., Stalling, D., Nadobny, J., et al, Three-dimensional finite element mesh generation for numerical simulations of hyperthermia treatments. In C. Franconi, G. Arcangeli, and R. Cavaliere (eds.), Proc. of the 7th Int. Congress on Hyperthermic Oncology, Rome, 1996.

8. Song, C. W., Lokshina, A., Rhee, J. G., Patten, M., Levitt, S. H., Implication of Blood Flow in Hyperthermic Treatment of Tumors. IEEE Trans. Biomed. Engrg., Vol. 31, 9 - 16, 1984.

9. Tompkins, D. T., et al, Temperature-dependent versus constant-rate blood perfusion modelling in ferromagnetic thermoseed hyperthermia: results with a model of the human prostate, Int. J. Hyperthermia, Vol. 10, No. 4, 517 - 536, 1994.

10. R. Beck, P. Deuflhard, H.-C. Hege, M. Seebaß, D. Stalling, Numerical Algorithms and Visualization in Medical Treatment Planning, Preprint SC 96-54, Konrad-Zuse-Zentrum für Informationstechnik Berlin, Germany, 1996.